

# A Predictive Approach to Assessing Microcephaly Risk in Zika Virus (ZIKV) Exposure

Jitendra Rajbhar<sup>1</sup>, A.K. Jaiswal<sup>2</sup>

<sup>1</sup>Research Scholar, Department of Mathematics and Statistics  
DDU, University Gorakhpur – 273001 (U.P.) India

<sup>2</sup>Professor, St. Andrew's College, Gorakhpur

## Abstract

A mathematical model based on integral equations has been developed and analyzed, which transforms into a dynamical system of nonlinear differential equations to assess the risk of microcephaly caused by the Zika virus. The model specifically considers a group of susceptible pregnant women. The epidemic threshold (basic reproduction number) was determined using the next-generation matrix method. Sensitivity analysis was conducted on the threshold with respect to each parameter. Lastly, multiple system simulations were performed to evaluate the incidence of exposure.

**Keywords:** Model, Microcephaly, Zika Virus, Basic Reproduction Number, Sensitivity Analysis

## 1. Introduction:

The Zika virus (ZIKV) is an arbovirus from the Flavivirus family, primarily transmitted by *Aedes aegypti* mosquitoes [1]. It was first identified in 1947 in a monkey in Uganda's Zika forest [2], with the earliest human cases reported in 1952 in Eastern Africa. Between 1977 and 1978, an outbreak occurred in Malaysia and Indonesia, attributed to an intense rainy season. Subsequently, cases re-emerged in 2007 on Yap Island in Micronesia [3][4]. The World Health Organization (WHO) and other health authorities in affected regions regard ZIKV as a significant public health concern, especially due to its association with favourable mosquito breeding conditions.

The increase in ZIKV cases due to climate change has also highlighted evidence of perinatal transmission, particularly in French Polynesia. Two such cases were documented: the first in December 2013, where a pregnant woman exhibited ZIKV symptoms two days before delivery, and the second in February 2014, where both the mother and newborn showed symptoms three and four days after delivery, respectively [5]. Additionally, evidence of sexual transmission has been reported, with cases identified in Southeastern Senegal in 2008 and during a ZIKV outbreak in Tahiti in 2013 [6][7].

A potential fourth transmission mechanism through blood transfusions has also been explored [8]. These findings collectively contribute to the growing number of people vulnerable to ZIKV.

The possibility of perinatal transmission warrants close analysis, as limited information exists on its potential impact on the central nervous system of fetuses or newborns. Comparatively, other arboviruses such as Chikungunya and Dengue have been associated with severe complications like encephalopathy, haemorrhagic fever, premature delivery, or fatal anomalies [5].

Furthermore, the WHO and the Brazilian Ministry of Health have raised concerns about a potential link between ZIKV and congenital microcephaly [4][9]. By November 21, 2015, 739 cases of microcephaly were reported across nine states in Brazil [9]. Although more evidence is required to confirm this connection, it has already posed a significant risk to pregnant women, exacerbated by the lack of a ZIKV vaccine.

Given the critical importance of these findings, a mathematical model based on nonlinear differential equations is proposed to describe ZIKV transmission dynamics, with a particular focus on a susceptible group of pregnant women.

## **2. Mathematical Model:**

A theoretical model based on non-linear ordinary differential equations has been introduced to describe the dynamics of population incidence among infected pregnant women who may present fetal microcephaly induced by the ZIKV virus. The model variables are defined as follows:  $S(t)$ , representing the average number of susceptible individuals;  $P(t)$ , the average number of ZIKV-infected pregnant women who may induce fetal microcephaly;  $I(t)$ , the average number of individuals infected by ZIKV;  $M_s(t)$ , the average number of non-carrier mosquitoes; and  $M_i(t)$ , the average number of virus-carrier mosquitoes. The total human population at time  $t$  is given by  $N_h(t) = S(t) + P(t) + I(t)$ , and the total mosquito population at time  $t$  is  $N_m(t) = M_s(t) + M_i(t)$ .

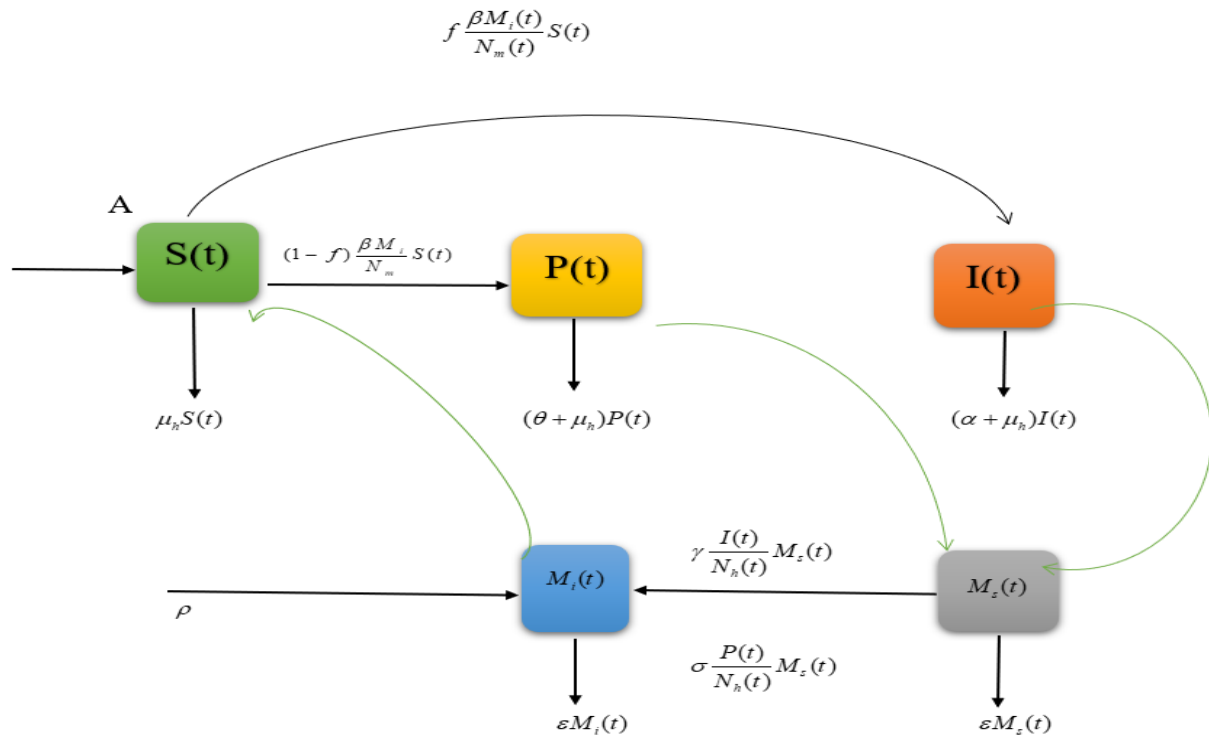


**Figure:1** Flow diagram of the dynamics.

The system of differential equations representing the infectious process is illustrated in Figure 1.

$$\frac{dS}{dt} = A - \frac{\beta M_i(t)}{N_m(t)} S(t) - \mu_h S(t) \dots\dots\dots(1)$$

$$\frac{dP}{dt} = (1-f) \frac{\beta M_i(t)}{N_m(t)} S(t) - (\theta + \mu_h) P(t) \dots\dots\dots(2)$$

$$\frac{dI}{dt} = f \frac{\beta M_i(t)}{N_m(t)} S(t) - (\alpha + \mu_h) I(t) \dots\dots\dots(3)$$

$$\frac{dM_s}{dt} = \rho - \frac{\sigma P(t)}{N_h(t)} M_s(t) - \frac{\gamma I(t)}{N_h(t)} M_s(t) - \epsilon M_s(t) \dots\dots\dots(4)$$

$$\frac{dM_i}{dt} = \sigma \frac{P(t)}{N_h(t)} M_s(t) + \frac{\gamma I(t)}{N_h(t)} M_s(t) - \epsilon M_i(t) \dots\dots\dots(5)$$

Where,  $A, \alpha, \mu_h, \theta, \rho, \epsilon > 0$   $0 < \beta, \sigma, \gamma, f < 1$  and the initial condition  $S(0) = S_0, P(0) = P_0, I(0) = I_0$  and  $M_s(0) = M_{s0}, M_i(0) = M_{i0}$ . By integrating equation (1) to (5), the trajectories were obtained:

$$S(t) = At - \beta \int_0^t \frac{M_i(s)S(s)}{N_m(s)} ds - \mu_h \int_0^t S(s) ds + S_0 \dots\dots\dots(6)$$

$$P(t) = (1 - f)\beta \int_0^t \frac{M_i(s)S(s)}{N_m(s)} ds - (\theta + \mu_h) \int_0^t P(s) ds + P_0 \dots\dots(7)$$

$$I(t) = f\beta \int_0^t \frac{M_i(s)S(s)}{N_m(s)} ds - (\alpha + \mu_h) \int_0^t I(s) ds + I_0 \dots\dots(8)$$

$$M_s(t) = \rho t - \sigma \int_0^t \frac{P(s)M_s(s)}{N_h(s)} ds - \gamma \int_0^t \frac{I(s)M_s(s)}{N_h(s)} ds - \varepsilon \int_0^t M_s(s) ds + M_{s0} \dots\dots(9)$$

$$M_i(t) = \sigma \int_0^t \frac{P(s)M_s(s)}{N_h(s)} ds + \gamma \int_0^t \frac{I(s)M_s(s)}{N_h(s)} ds - \varepsilon \int_0^t M_s(s) ds + M_{i0} \dots\dots(10)$$

The trajectories represent the solutions for each population, as demonstrated in the simulations.

**Table 1:** Table of Description

Variable and Parameters	Description Susceptible
A	Constant flux of susceptible individuals.
$\mu_h$	Natural death rate of people.
$\beta$	Probability of virus transmission from virus-carrier mosquitoes to susceptible individuals.
$\sigma$	Probability of virus transmission from infected pregnant women to non-carrier mosquitoes.
$\gamma$	Probability of virus transmission from infected individuals to non-carrier mosquitoes.
$\varepsilon$	Adult mosquito death rate.
$\theta$	Recovery rate of infected pregnant Women.
$\alpha$	Recovery rate of infected individuals.
f	fraction of infected individuals.
(1 - f)	fraction of pregnant women infected by ZIKV.

### 3. Boundedness of the system:

This will describe conditions under which the solutions of the system remain bounded.

**Theorem:** For the given differential equations system (1) to (5), if the parameters,  $A, \alpha, \mu_h, \theta, \rho, \varepsilon > 0$  and  $0 < \beta, \sigma, \gamma, f < 1$ , then the solutions  $(S(t), P(t), I(t), M_s(t), M_i(t))$  are bounded for all  $t \geq 0$ , provided that the initial conditions  $S(0) = 0, P(0) = 0, I(0) = 0, M_s(0) = 0, M_i(0) = 0$  are finite and non-negative.

**Proof:** Since all the parameters are non-negative, and the equations describe physical quantities (e.g., populations or densities), the solutions are non-negative if the initial conditions are non-negative. Using the form of  $\frac{dS}{dt}, \frac{dP}{dt}, \frac{dI}{dt}, \frac{dM_s}{dt}, \frac{dM_i}{dt}$  it is clear that no negative feedback mechanism exists that would lead to negative values starting from non-negative initial conditions.

Define the total population as:

$$N(t) = S(t) + P(t) + I(t) + M_s(t) + M_i(t) \dots\dots\dots(11)$$

Taking the time derivative:

$$\frac{dN(t)}{dt} = \frac{dS}{dt} + \frac{dP}{dt} + \frac{dI}{dt} + \frac{dM_s}{dt} + \frac{dM_i}{dt}$$

Substitute the given equations (1) to (5) into this expression. After simplifications:

$$\frac{dN(t)}{dt} \leq A + \rho - \mu_h S(t) - (\theta + \mu_h)P(t) - (\alpha + \mu_h)I(t) - \varepsilon M_s(t) - \varepsilon M_i(t)$$

Since  $A, \mu_h, \alpha, \varepsilon > 0$ , this shows that the growth of  $N(t)$  is bounded above.

Construct a Lyapunov function:

$$V(t) = S(t) + P(t) + I(t) + M_s(t) + M_i(t) \dots\dots\dots(12)$$

Its derivative is bounded as shown earlier. Using LaSalle's invariance principle, the system will remain bounded.

**Upper Bound:** Integrate the inequality for  $\frac{dN(t)}{dt}$  to show that:

$$N(t) \leq N(0) + \frac{A}{\min(\mu_h, \alpha, \varepsilon)}$$

Thus, all components  $S(t), P(t), I(t), M_s(t), M_i(t)$  are individually bounded.

This theorem and proof ensure that the solutions to the system are bounded under the given conditions.

#### 4. Analysis of Equilibria:

In this analysis, two equilibrium points of the system were identified: the disease-free equilibrium (DFE) and the disease-endemic equilibrium (DEE). The DFE occurs when the basic reproduction number ( $R_0$ ) is less than one ( $R_0 < 1$ ), while the DEE arises when the basic reproduction number exceeds one ( $R_0 > 1$ ).

#### 4.1 Disease-Free Equilibrium (DFE):

The disease-free equilibrium corresponds to the state where the infectious components of the population  $(P(t), I(t), M_s(t), M_i(t))$  vanish, leaving only the uninfected population  $S(t)$  in the system.

At DFE:

$$P^* = 0, I^* = 0, M_s^* = 0, M_i^* = 0$$

Substituting these into the system:

$$\frac{dS}{dt} = A - \mu_h S = 0 \Rightarrow S^* = \frac{A}{\mu_h}$$

Thus, the disease-free equilibrium (DFE) is

$$(S^*(t), P^*(t), I^*(t), M_s^*(t), M_i^*(t)) = \left( \frac{A}{\mu_h}, 0, 0, 0, 0 \right)$$

#### 4.2 Endemic Equilibrium (EE):

The endemic equilibrium occurs when the disease persists in the population, i.e.,  $P^*(t), I^*(t), M_s^*(t), M_i^*(t) > 0$ . To find the endemic equilibrium, we solve the system at steady state

$$\left( \frac{dS}{dt} = \frac{dP}{dt} = \frac{dI}{dt} = \frac{dM_s}{dt} = \frac{dM_i}{dt} = 0 \right).$$

#### Steady-State Equations:

From the equilibrium equations

$$A - \beta \frac{M_i^*(t)}{N_m^*(t)} S^*(t) - \mu_h S^*(t) = 0 \Rightarrow S^*(t) = \frac{A}{\mu_h + \beta \frac{M_i^*(t)}{N_m^*(t)}}$$

$$(1-f) \beta \frac{M_i^*(t)}{N_m^*(t)} S^*(t) - (\theta + \mu_h) P^*(t) = 0 \Rightarrow P^*(t) = \frac{(1-f) \beta \frac{M_i^*(t)}{N_m^*(t)} S^*(t)}{\theta + \mu_h}$$

$$f \beta \frac{M_i^*(t)}{N_m^*(t)} S^*(t) - (\alpha + \mu_h) I^*(t) = 0 \Rightarrow I^*(t) = \frac{f \beta \frac{M_i^*(t)}{N_m^*(t)} S^*(t)}{\alpha + \mu_h}$$

$$\rho - \sigma \frac{P^*(t)}{N_h^*(t)} M_s^*(t) - \gamma \frac{I^*(t)}{N_h^*(t)} M_s^*(t) - \varepsilon M_s^*(t) = 0 \Rightarrow M_s^*(t) = \frac{\rho}{\sigma \frac{P^*(t)}{N_h^*(t)} + \frac{\gamma I^*(t)}{N_h^*(t)} + \varepsilon}$$

$$\sigma \frac{P^*(t)}{N_h^*(t)} M_s^*(t) + \frac{\gamma I^*(t)}{N_h^*(t)} M_s^*(t) - \varepsilon M_i^*(t) = 0 \Rightarrow M_i^*(t) = \frac{\sigma \frac{P^*(t)}{N_h^*(t)} M_s^*(t) + \frac{\gamma I^*(t)}{N_h^*(t)} M_s^*(t)}{\varepsilon}$$

Here,  $N_m^*(t) = M_s^*(t) + M_i^*(t)$  and  $N_h^*(t) = S^*(t) + P^*(t) + I^*(t)$ .

### 5. Stability Analysis:

Considering an average temperature of approximately 23°C in Armenia (Quindío), we have calculated the transmission probabilities  $\gamma$ ,  $\beta$  and  $\epsilon$  using the formulas provided in references [10] and [11].

$$\gamma = 0.0729T - 0.9037, 12.4^\circ C \leq T \leq 26.1^\circ C \dots (13)$$

$$\beta = 0.001044T(T - 12.286)(32.461 - T)^{\frac{1}{2}}, 12.4^\circ C \leq T \leq 26^\circ C \dots (14)$$

$$\epsilon = 0.8692 - 0.1590T + 0.01116T^2 - 0.0003408T^3 + 0.000003809T^4 \dots (15)$$

Where  $10.54^\circ C \leq T \leq 33.4^\circ C$ , the parameters  $\mu_h$  and  $\theta$  were estimated based on the Poisson process theory in epidemiology [2]. Specifically,  $E[P(t)] = \frac{1}{\theta + \mu_h}$ , incorporating a life expectancy of 75 years in Colombia and an average the transmissibility period was considered to be 7 days (E[x]) [2]. The parameter values  $\sigma$  and  $\alpha$  were assigned based on previously reported values, as detailed in Table 1.

The local stability analysis of the model was performed using the data presented in Table 1. The process began with the calculation of the equilibrium points for both the infection-free state and the prevalence state.

These equilibrium points were determined by solving the following nonlinear algebraic system.

$$20 - (0.7913) \frac{M_i(t)}{M_s(t) + M_i(t)} S(t) - (0.0003) S(t) = 0 \dots (16)$$

$$(1 - f)(0.7913) \frac{M_i(t)}{M_s(t) + M_i(t)} S(t) - (0.05 + 0.0003) P(t) = 0 \dots (17)$$

$$f(0.7913) \frac{M_i(t)}{M_s(t) + M_i(t)} S(t) - (0.14 + 0.0003) I(t) = 0 \dots (18)$$

$$30 - (0.6) \frac{P(t)}{S(t) + P(t) + I(t)} M_s(t) - (0.773) \frac{I(t)}{S(t) + P(t) + I(t)} M_s(t) - (0.0352) M_s(t) = 0 \dots (19)$$

$$(0.6) \frac{P(t)}{S(t) + P(t) + I(t)} M_s(t) + (0.773) \frac{I(t)}{S(t) + P(t) + I(t)} M_s(t) - (0.0352) M_i(t) = 0 \dots (20)$$

Using the MAPLE software, the equilibrium points listed in Table 2 were determined. To linearize the nonlinear system described by equations (1) to (5), we computed the Jacobian matrix at the generic equilibrium point

$$E = \left( \hat{S}(t), \hat{P}(t), \hat{I}(t), \hat{M}_s(t), \hat{M}_i(t) \right),$$

$$J = \begin{bmatrix} f_{S(t)} & 0 & 0 & f_{S(t)} & f_{M_i(t)} \\ -(1-f)(f_{S(t)} + \mu_h) & -(\mu_h + \theta) & 0 & -(1-f)f_{M_s(t)} & -(1-f)f_{M_i(t)} \\ -(f_{S(t)} + \mu_h)f & 0 & -(\mu_h + \alpha) & -ff_{M_s(t)} & -ff_{M_i(t)} \\ w_{S(t)} & w_{P(t)} & w_{I(t)} & w_{M_s(t)} & 0 \\ -w_{S(t)} & -w_{P(t)} & -w_{I(t)} & -(w_{M_s(t)} + \varepsilon) & -\varepsilon \end{bmatrix}$$

Where,  $f_{S(t)} = -\beta \frac{\hat{M}_i(t)}{\hat{N}_m(t)} - \mu_h$ ,  $f_{M_s(t)} = \beta \frac{\hat{M}_i(t)\hat{S}(t)}{(\hat{M}_s(t) + \hat{M}_i(t))^2}$ ,  $f_{M_i(t)} = -\beta \frac{\hat{M}_i(t)\hat{S}(t)}{(\hat{M}_s(t) + \hat{M}_i(t))^2}$

$$w_{S(t)} = \frac{\sigma \hat{P}(t)\hat{M}_s(t)}{(\hat{N}_h(t))^2} + \frac{\gamma \hat{I}(t)\hat{M}_s(t)}{(\hat{N}_h(t))^2}, w_{P(t)} = \frac{\sigma (\hat{S}(t) + \hat{I}(t))\hat{M}_s(t)}{(\hat{N}_h(t))^2} + \frac{\gamma \hat{I}(t)\hat{M}_s(t)}{(\hat{N}_h(t))^2}$$

$$w_{I(t)} = \frac{\sigma \hat{P}(t)\hat{M}_s(t)}{(\hat{N}_h(t))^2} + \frac{\gamma (\hat{S}(t) + \hat{P}(t))}{(\hat{N}_h(t))^2}, w_{M_s(t)} = -\frac{\sigma \hat{P}(t)}{(\hat{N}_h(t))^2} - \frac{\gamma \hat{I}(t)}{(\hat{N}_h(t))^2} - \varepsilon$$

Using the data from Table 2 and the identified equilibrium points, a local stability analysis is conducted. By applying the Jacobian matrix, the following results are obtained.

Table 3 provides a summary of the local stability analysis for the dynamic system (1–5) in relation to the fraction of infected women. For each equilibrium point, the eigenvalues are presented, illustrating the stability based on the epidemic threshold ( $R_0$ ).

**Table 2:** Parameters Values

Parameter	$\alpha$	$\beta$	$\gamma$	$\sigma$	$\varepsilon$	$\mu_h$	$\theta$	$\rho$	$A$	$f$
Value	0.14	0.7913	0.773	0.6	0.0352	0.0003	0.05	30	20	0.3,0.6,0.85,1

**Table 3:** Analyzing the local stability of the system for each  $f$ .

$f$	Equilibrium point	Eigenvalues	Stability	Threshold ( $R_0$ )
0.3	(66667, 0, 0, 857, 0)	0.67, -0.0002, -0.070, -0.107, -0.761	Unstable	14.9869
0.3	(27, 278, 43, 49, 808)	-0.035, -0.050, -0.140, -0.595, -0.761	Stable	14.9869
0.6	(66667, 0,0, 857, 0)	0.693, -0.0003, -0.070, -0.080, -0.803	Unstable	13.4672
0.6	(27, 159, 86, 48, 810)	-0.035, -0.050, -0.140, -0.608, -0.769	Stable	13.4672
0.85	(66667, 0,0, 857, 0)	0.7065, -0.0002, -0.061, -0.070, -0.836	Unstable	12.0555
0.85	(27, 60, 121, 46, 812)	0.0349, -0.005, -0.140, -0.625, -0.781	Stable	12.0555
1	(66667, 0, 851, 0)	0.714, -0.0002, -0.0703, -0.8540	Unstable	11.1227
1	(27, 143, 44, 808)	-0.0348, -0.1404, -0.6424, -0.7952	Stable	11.1227

**6. Basic Reproduction Number ( $R_0$ )**

The epidemic threshold ( $R_0$ ), represents the average number of secondary cases produced by an infected individual during their infectious period within a fully susceptible population [12][13]. This value is determined using the next-generation matrix method [13][14]. To calculate it, we revisit the dynamic system (1–5) as follows:

$$\frac{dP(t)}{dt} = (1-f)\beta \frac{M_i(t)}{N_m(t)} S(t) - (\theta + \mu_h)P(t) \dots\dots\dots (21)$$

$$\frac{dI(t)}{dt} = f \frac{\beta M_i(t)}{N_m(t)} S(t) - (\alpha + \mu_h) I(t) \quad \dots\dots\dots (22)$$

$$\frac{dM_i(t)}{dt} = \sigma \frac{P(t)}{N_h(t)} M_s(t) + \frac{\gamma I(t)}{N_h(t)} M_s(t) - \varepsilon M_i(t) \quad \dots\dots\dots (23)$$

$$\frac{dM_s(t)}{dt} = \rho - \frac{\sigma P(t)}{N_h(t)} M_s(t) - \frac{\gamma I(t)}{N_h(t)} M_s(t) - \varepsilon M_s(t) \quad \dots\dots\dots (24)$$

$$\frac{dS(t)}{dt} = A - \frac{\beta M_i(t)}{N_m(t)} S(t) - \mu_h S(t) \quad \dots\dots\dots (25)$$

From the first three equations describing the infectious process, the matrices were derived.

$$F = \begin{bmatrix} 0 & 0 & \frac{(1-f)\beta A \varepsilon}{\mu_h \rho} \\ 0 & 0 & \frac{f \beta A \varepsilon}{\mu_h \rho} \\ \frac{\sigma \rho \mu_h}{\varepsilon A} & \frac{\gamma \rho \mu_h}{\varepsilon A} & 0 \end{bmatrix} \text{ and } V = \begin{bmatrix} \theta + \mu_h & 0 & 0 \\ 0 & \alpha + \mu_h & 0 \\ 0 & 0 & \varepsilon \end{bmatrix} \quad \text{Then}$$

$$V^{-1} = \frac{1}{(\theta + \mu_h)(\alpha + \mu_h)\varepsilon} \begin{bmatrix} \varepsilon(\alpha + \mu_h) & 0 & 0 \\ 0 & \varepsilon(\theta + \mu_h) & 0 \\ 0 & 0 & (\alpha + \mu_h)(\theta + \mu_h) \end{bmatrix}$$

$$\Rightarrow F = \begin{bmatrix} 0 & 0 & \frac{(1-f)\beta A \varepsilon}{\mu_h \rho} \\ 0 & 0 & \frac{f \beta A \varepsilon}{\mu_h \rho} \\ \frac{\sigma \rho \mu_h}{\varepsilon A} & \frac{\gamma \rho \mu_h}{\varepsilon A} & 0 \end{bmatrix} \text{ and } V^{-1} = \begin{bmatrix} \frac{1}{\theta + \mu_h} & 0 & 0 \\ 0 & \frac{1}{\alpha + \mu_h} & 0 \\ 0 & 0 & \frac{1}{\varepsilon} \end{bmatrix} \quad \dots\dots\dots (26)$$

And the resulting next-generation matrix,

$$\Omega = FV^{-1} = \begin{bmatrix} 0 & 0 & \frac{(1-f)\beta A}{\mu_h \rho} \\ 0 & 0 & \frac{f\beta A}{\mu_h \rho} \\ \frac{\sigma \rho \mu_h}{\varepsilon A(\theta + \mu_h)} & \frac{\gamma \rho \mu_h}{\varepsilon A(\alpha + \mu_h)} & 0 \end{bmatrix} \dots\dots\dots (27)$$

Which possesses a characteristic equation in the form,

$$\lambda \left[ \lambda^2 + \frac{(1-f)\beta\sigma}{\varepsilon(\theta + \mu_h)} + \frac{f\gamma\beta}{\varepsilon(\alpha + \mu_h)} \right] = 0 \dots\dots\dots (28)$$

Along with its eigenvalues,

$$\lambda_1 = 0, \lambda_{2,3} = \pm \sqrt{\frac{(1-f)\beta\sigma}{\varepsilon(\theta + \mu_h)} + \frac{f\gamma\beta}{\varepsilon(\alpha + \mu_h)}} \dots\dots\dots (29)$$

Thus, the spectral radius (the dominant eigenvalue) is

$$R_0(f) = \rho(\Omega) = \max\{\lambda_1, \lambda_2, \lambda_3\} = \sqrt{\frac{(1-f)\beta\sigma}{\varepsilon(\theta + \mu_h)} + \frac{f\gamma\beta}{\varepsilon(\alpha + \mu_h)}} \dots\dots\dots (30)$$

Local sensitivity is a relative measure of how a variable responds to changes in a parameter [15]–[17]. The sensitivity index for ( $R_0$ ) is determined using the following formula:

$$I_p^{R_0} = \frac{\partial R_0}{\partial p} \times \frac{p}{R_0} \dots\dots\dots (31)$$

Here, p represents a parameter. From this equation, the following indices are derived,

$$I_\beta^{R_0} = 0.5$$

$$I_\gamma^{R_0} = \frac{f\gamma(\theta + \mu_h)}{2(1-f)\sigma(\alpha + \mu_h) + f\gamma(\theta + \mu_h)}$$

$$I_\varepsilon^{R_0} = -0.5$$

$$I_\alpha^{R_0} = \frac{\alpha f \gamma}{\alpha + \mu_h} \left[ \frac{\theta + \mu_h}{(1-f)\sigma(\alpha + \mu_h) + f\gamma(\theta + \mu_h)} \right]$$

$$I_{\mu_h}^{R_0} = \frac{\mu_h}{2} \left[ \frac{(1-f)\sigma}{(\theta + \mu_h)^2} + \frac{f\gamma}{(\theta + \mu_h)^2} \right] \left[ \frac{(\theta + \mu_h)(\alpha + \mu_h)}{(1-f)\sigma(\alpha + \mu_h) + f\gamma(\theta + \mu_h)} \right]$$

$$I_f^{R_0} = -\frac{f\sigma(\alpha + \mu_h) - f\gamma(\theta + \mu_h)}{2(1-f)\sigma(\alpha + \mu_h) + 2f\gamma(\theta + \mu_h)}$$

$$I_\sigma^{R_0} = \frac{(1-f)\sigma(\alpha + \mu_h)}{2(1-f)\sigma(\alpha + \mu_h) + 2f\gamma(\theta + \mu_h)}$$

$$I_\rho^{R_0} = -\frac{(1-f)\sigma\theta}{2(\theta + \mu_h)} \left[ \frac{\alpha + \mu_h}{(1-f)\sigma(\alpha + \mu_h) + f\gamma(\theta + \mu_h)} \right]$$

The sensitivity values for each parameter are presented. It is evident that  $R_0$  is directly proportional to the recovery rate of infected individuals  $\alpha$ . Similarly, an increase in the adult mosquito death rate leads to a decrease in  $R_0$ , demonstrating that strategies aimed at raising mosquito mortality can effectively reduce the incidence of ZIKV and, consequently, the risk of microcephaly.

### 7. Simulations and Discussion:

The simulations for systems (1) to (5) were conducted using the data provided in Table 2 and analyzed with the MAPLE software. The first graph in Figure 2 illustrates an almost linear relationship between  $R_0$  and the proportion of infected individuals ( $f$ ) within the range  $f \in [0.3, 1]$ . The right section of Figure 2 displays the sensitivity indices for each parameter, represented as individual lines.

**Table 4:** Sensitivity indices of  $R_0$  as a function of each parameter.

Parameter	$\alpha$	$\beta$	$\gamma$	$\sigma$	$\varepsilon$	$\theta$	$\rho$	$\mu_h$	$A$	$f$
$I_p^{R_0}$	0.7220	0.5000	0.5668	0.1382	-0.50	- 0.1373	-	0.00002	-	-

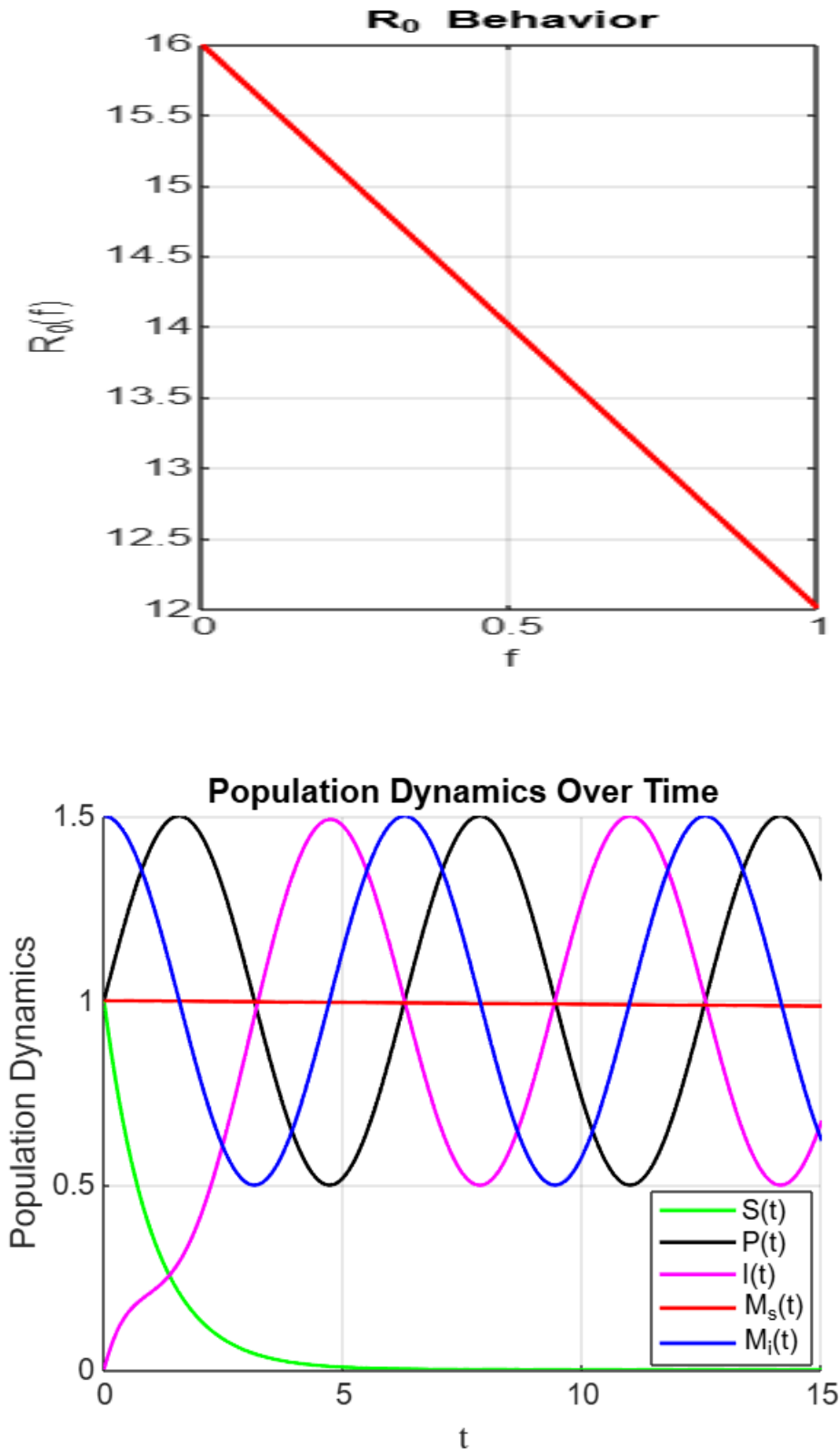


**Figure 2:** The behaviour of  $R_0$  and the local sensitivity index  $I_p^{R_0}$  are illustrated with the following colour representations:  $\alpha$  (black line),  $\beta$  (orange line),  $\gamma$  (blue line),  $\mu_h$  (red line),  $f$  (green line),  $\rho$  (brown line), and  $\varepsilon$  (leaf green line).

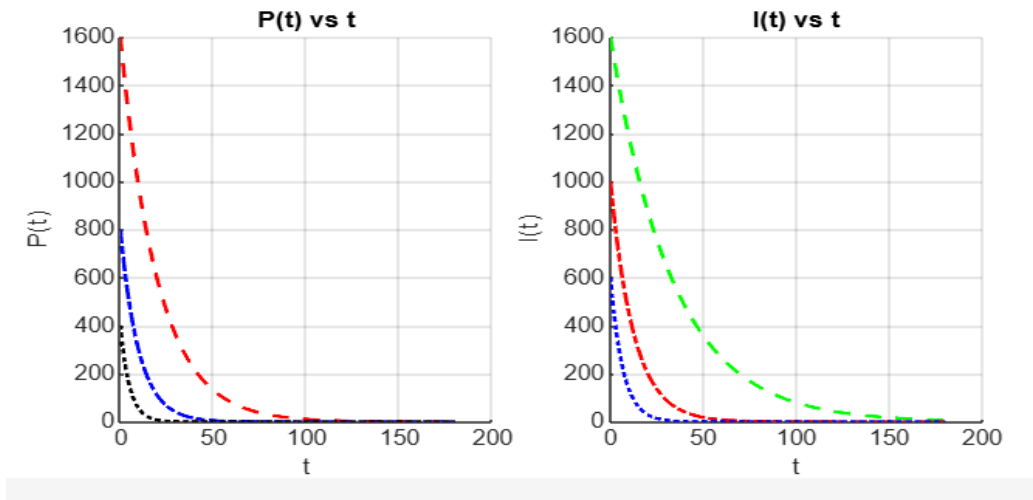


**Figure 3:** Dynamics of infected pregnant women  $P(t)$  and individuals  $I(t)$  affected by the Zika virus.

In **Figure 3**, it is evident that as  $f$  increases, the population of infected pregnant women reaches a significant epidemic peak within the first 10 days. In the absence of infections among pregnant women, the ZIKV incidence is approximately 1700 cases every 10 days. Over a period of 80 days, the populations tend to stabilize.

For the rest of the infected population, a similar trend is observed, with minor variations in the epidemic peaks. This population stabilizes at values below 200 individuals within approximately 40 days.

Finally, **Figure 4** illustrates the trajectories of the infectious process for a small fraction of pregnant women infected with ZIKV. Assuming a potential link between ZIKV infection and microcephaly, the proposed model highlights the risk of fetal exposure leading to the development of microcephaly.

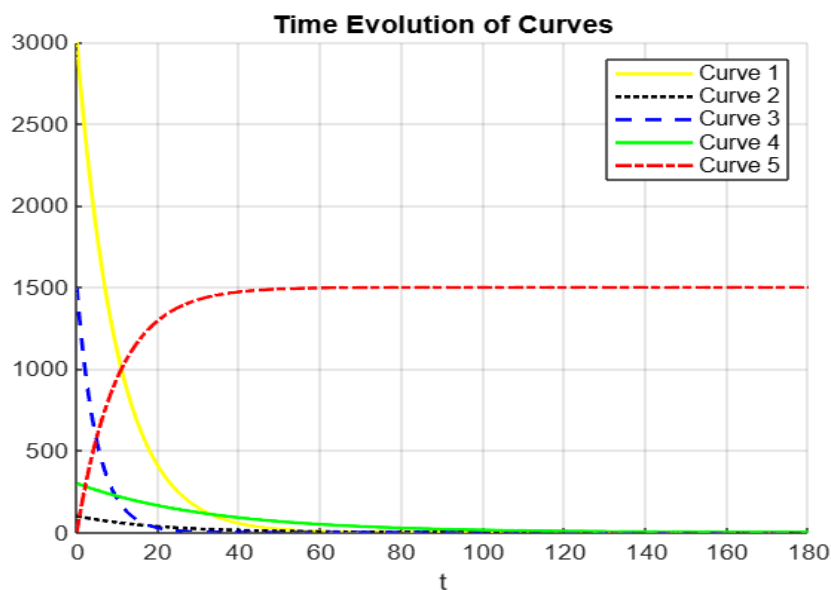


**Figure 4:** Dynamics of populations with  $f = 0.85$ .

## 8. Conclusion

From the analysis of the proposed model, it is evident that the dynamics of Zika Virus (ZIKV) transmission are significantly influenced by the acquisition of the infection among pregnant women and the subsequent risk of fatal exposure. This highlights the critical need for a comprehensive understanding of how changes in the fraction of pregnant women acquiring ZIKV directly impact fatal health outcomes, including the potential for severe congenital conditions such as microcephaly and other neurological complications.

The findings underscore the importance of considering both biological and behavioural factors when modelling ZIKV transmission. For example, pregnant women form a vulnerable subpopulation due to the dual risk posed to both maternal and fetal health. This necessitates tailored interventions and preventative strategies that specifically target this group, including community-based education campaigns, improved access to healthcare, and monitoring during pregnancy.

Moreover, the dynamics of ZIKV transmission emphasize the urgent need for integrated control strategies to combat the primary vector, *Aedes* mosquitoes. Measures such as environmental sanitation, elimination of mosquito breeding sites, and use of insecticides are foundational. However, these must be supplemented by innovative solutions such as the introduction of genetically modified mosquitoes, biological control agents (e.g., *Wolbachia*-infected mosquitoes), and the promotion of mosquito-repellent technologies. Furthermore, individual-level precautions, including the use of insect-repellent clothing and treated nets, must be actively promoted, especially among pregnant women in endemic regions.

In the context of preventing pregnancy during outbreaks, it is critical to incorporate reproductive health measures into public health policies. This involves promoting family planning services and ensuring widespread availability of contraceptives, including emergency contraceptives. Empowering women and couples to make informed decisions about pregnancy during outbreaks is crucial for reducing fatal exposure risks. Public health authorities must also prioritize communication strategies to provide clear and culturally sensitive guidance on the risks of ZIKV during pregnancy and the available preventive options.

Looking ahead, the development and dissemination of vaccines against ZIKV present a promising avenue to reduce the burden of the disease. Continued investment in research and development is essential to make vaccines widely available, particularly in regions where ZIKV outbreaks are recurrent. Additionally, integrating vaccination campaigns with vector-control programs can amplify the impact and help achieve long-term control of the disease.

Finally, robust surveillance systems are pivotal for understanding the spatiotemporal dynamics of ZIKV transmission and predicting future outbreaks. Such systems must incorporate data on environmental conditions, vector density, human mobility patterns, and reproductive health statistics to enable targeted and timely interventions. Multidisciplinary approaches that bridge epidemiology, public health, and social sciences are essential for designing and implementing effective policies.

In conclusion, the proposed model provides critical insights into the interplay between ZIKV transmission, pregnant women's exposure, and fatal risks. The results underline the need for a multipronged strategy that includes vector control, reproductive health measures, and innovative research efforts. By integrating these approaches, public health systems can better protect vulnerable populations, minimize fatal exposure risks, and ultimately reduce the societal burden of ZIKV outbreaks. Such comprehensive strategies are vital for building resilient healthcare systems capable of responding to emerging infectious diseases in the future.

## 9. References:

- [1] Musso, D., Nilles, E.J., and Cao-Lormeau, V.M. (2014). Rapid Spread of Emerging Zika Virus in the Pacific Area. *Clinical Microbiology and Infection*, 20, O595-O596. <http://dx.doi.org/10.1111/1469-0691.12707>
- [2] Rodrigez, A.J. (2015). Zika: The New Arbovirus Threat for Latin America. *The Journal of Infection in Developing Countries*, 9, 684-685.
- [3] Duffy, M.R., Chen, T.H., Hancock, W.T., et al. (2009). Zika Outbreak on Yap Island, Federated States of Micronesia. *The New England Journal of Medicine*, 366, 2536-2543. <http://dx.doi.org/10.1056/NEJMoa0805715>
- [4] Gatherer, D., and Kohl, A. (2015). Zika Virus: A Previously Slow Pandemic Spreads Rapidly through the Americas. *Journal of General Virology*, 97, 269-273. <http://dx.doi.org/10.1099/jgv.0.000381>
- [5] Besnard, M., Lastere, S., Teissier, A., Cao-Lormeau, V., and Musso, D. (2014). Evidence of Perinatal Transmission of Zika Virus. French Polynesia, December 2013 and February 2014. *Eurosurveillance*, 19, 20751. <http://dx.doi.org/10.2807/1560-7917.ES2014.19.13.20751>
- [6] Foy, B.D., Kobylinski, K.C., Chilson Foy, J.L., Blitvich, B.J., Travassos da Rosa, A., Haddow, A.D., et al. (2011). Probable Non-Vector-Borne Transmission of Zika Virus, Colorado, USA. *Emerging Infectious Diseases*, 17, 880-882. <http://dx.doi.org/10.3201/eid1705.101939>
- [7] Didier, M., Claudine, R., Emilie, R., Tuxuan, N., Anita, T., and Van Mai, C.L. (2015). Potential Sexual Transmission of Zika Virus. *Emerging Infectious Diseases*, 21.
- [8] Baud, D., Gubler, D.J., Schaub, B., Lanteri, M.C., and Musso, D. (2017). An Update on Zika Virus Infection. *The Lancet*, 390(10107), 2099-2109. [https://doi.org/10.1016/S0140-6736\(17\)31450-2](https://doi.org/10.1016/S0140-6736(17)31450-2)
- [9] Petersen, E.E., Staples, J.E., Meaney-Delman, D., et al. (2016). Interim Guidelines for Pregnant Women During a Zika Virus Outbreak — United States, 2016. *Morbidity and Mortality Weekly Report (MMWR)*, 65(2), 30-33. <https://doi.org/10.15585/mmwr.mm6502e1>
- [10] Mlakar, J., Korva, M., Tul, N., et al. (2016). Zika Virus Associated with Microcephaly. *The New England Journal of Medicine*, 374(10), 951-958. <https://doi.org/10.1056/NEJMoa1600651>
- [11] Ribeiro, G.S., and Kitron, U. (2019). Zika Virus Pandemic: A Public Health and Research Challenge. *The Journal of Clinical Investigation*, 129(5), 2165-2173. <https://doi.org/10.1172/JCI124134>



[12] World Health Organization (WHO). (2016). Zika Virus and Complications: Questions and Answers. <https://www.who.int/news-room/q-a-detail/zika-virus>